CATALYTIC CONVERSION OF CO to CO_2 WITH OXIDE NANOCATALYSTS: RADIATION EFFECT ON THE CO OXIDATION PROCESS

[1]S.H. Hasanov, [2*]H.Kh. Khalilova, [2]N.N. Musayeva, [3]N.M. Hasanguliyeva

[1]SOCAR, "Azneft" Production Union, Neftchiler ave., 73, AZ 1004, Baku, Azerbaijan
[2]Institute of Physics Public Legal Entity, Ministry of Science and Education of the Republic of Azerbaijan, H. Javid ave., 131, AZ 1143 Baku, Azerbaijan
[3]Institute of Chemistry Public Legal Entity, Ministry of Science and Education of the Republic of Azerbaijan, H. Javid ave., 113, AZ 1143 Baku, Azerbaijan
e-mail: khalilovaecology@gmail.com

Received 21.01.2026
Accepted 24.03.2026

Abstract: *Nanostructured Al_2O_3 and CuO oxides have been used in the decontamination of a hazardous gas – carbon monoxide (CO) - through heterogeneous catalysis. The structural and morphological characteristics of the nanoparticles were investigated by XRD, FT-IR, SEM, and TEM analyses. The process of CO oxidation to CO_2 was studied using three types of nanocatalysts, including Al_2O_3, Al_2O_3/12%CuO composite and radiation modified Al_2O_3/12%CuO composite. The process was thermally investigated, comparing with the results obtained on the surface of the nano-catalyst modified by gamma radiation. The results derived from the investigation have shown that the oxidation of CO on the surface of modified Al_2O_3/CuO nanocomposite irradiated in air by gamma rays increased by 6-8% due to the oxide-anion centers formed on the catalyst surface under the influence of gamma rays. The activity, stability, and formation of additional anion-hole centers in the oxidation process and the structural changes obtained through reduction processes of the nanocatalyst in catalytic and chemical reactions were studied. The kinetics and mechanism of the process are discussed.*

Keywords: *oxide nanocatalyst, carbon monoxide, heterogenous catalysis, nanocomposite, gamma radiation*

Introduction

Since the last decades of the 20th century, a huge amount of hazardous pollutants have been emitted to the atmosphere, disturbing the ecological balance worldwide. According to the information of the World Health Organization, 7 million deaths occur yearly due to air pollution. In countries with developed industrial and transport infrastructure, the main atmosphere emissions are nitrogen oxides (NO, NO_x, etc.), carbon oxides (CO, CO_2), sulfur oxide (SO_2), hydrogen sulfide (H_2S), hydrocarbons (C_xH_y) and solid particulate matter [1, 2].

Carbon monoxide (CO) has very toxic effect for human health among the gaseous substances. It can be generated from vehicles and industrial sources as a result of the incomplete combustion of fossil fuels and is one of the main components of the exhaust gases. Due to the increasing number of automobiles, the volume of CO emissions has reached a crucial level in urban areas. Carbon monoxide affects the nervous and cardiovascular systems. When the CO content in the air we breathe is 0.1%, death may occur within 30-60 minutes and when the CO content is 1% or more – instantly [3]. To prevent the negative effects of CO, it should either be captured or converted to non-toxic compounds.

Converting CO into less harmful gas – carbon dioxide (CO_2) through catalytic oxidation is of great importance in view of avoiding the consequent undesirable incidents. Gas-solid heterogeneous catalytic methods have been extensively investigated for CO oxidation. It has been reported that most of the noble metals (Pd, Pt, Au and Rh) can show high activity for catalytic CO oxidation due to their high catalytic activity and high resistance to sintering [4-6]. However, the high price and restricted availability of these metals hinder their widespread application. Therefore, preparation of more economically suitable catalysts is of great importance. Various metal oxide-based catalysts including semiconductors, hopcalites, spinel, and perovskite structure materials have been used to initiate CO oxidation reaction [7-10]. Oxide catalysts with the cations of transition metals are of great importance

for environmental applications. In recent decades, Cu-based composite materials have been extensively studied and reported by authors. Solid catalysts containing CuO exhibit good performance in the decontamination of hydrocarbons, volatile organic compounds (VOCs), CO and NO_x [11-16].

Catalysts based on nanostructured metal compounds promote CO oxidation at low temperatures [5, 8, 16, 17]. The development of more stable nanocatalysts is very important to achieve efficient results. Small nanoparticles are catalytically active due to their high surface areas. But they are not stable and can form larger particles. To increase the stability of nanocatalysts, the impregnation of catalytically active nanostructures into mesoporous structures is one of the reasonable ways. This can be done either during the synthesis of catalytic structures or the deposition of nanoparticles onto the mesoporous structures. There are various methods such as atomic layer deposition, supercritical fluid deposition, etc. used by authors for the incorporation of metal nanoparticles of mesoporous oxide catalysts [13, 18, 19].

Radiation of mixed nanocatalysts (like Al_2O_3+CuO, Pd-Cu/Al_2O_3) significantly enhances CO oxidation by creating active anion centers and oxygen vacancies, intensifying CO conversion rates, mostly at lower temperatures, often by lowering activation energy and forming reactive oxygen species [20, 21]. This radiation-induced activation creates synergistic effects, promoting faster reactions through electronic modifications and increased surface oxygen availability. The radiation deposition method uses a large surface area for dispersed active sites and confinement effects. Mesoporous Al_2O_3 provides a high surface area preventing nanoparticle agglomeration and improving mass/heat transfer.

Previously, we investigated the neutralization of NO_x and CO gases using γ-Al_2O_3 catalyst in combination with 12% transition metal oxides such as CoO, NiO and CuO. The data derived from investigations have shown that CuO-contained catalysts demonstrated higher activity in the neutralization of NO_x and CO gases compared to CoO- and NiO-containing catalysts [22].

The present work provides the results of our studies addressing the characterization of CuO and Al_2O_3 nanoparticles we synthesized in laboratory conditions and their application in converting CO gas to CO_2 through heterogeneous catalysis.

Experimental part

Materials. The Al_2O_3 and CuO nanoparticles (NPs) used in our experiments were synthesized by a simple sol-gel method. The chemical reagents used in the experiments were aluminum chloride ($AlCl_3$), copper chloride hexahydrate ($CuCl_2 \cdot 6H_2O$), sodium hydroxide (NaOH), citric acid ($C_6H_8O_7 \cdot H_2O$), cadmium chloride ($CdCl_2$). Nitric acid HNO_3 (65%) was used for mass spectral analysis [23].

To prepare the Al_2O_3/12% CuO composite, the synthesized CuO nanoparticles, in the amount of 12 mass% was mixed with the synthesized Al_2O_3 nanoparticles. After the particles are crushed and mixed well together until a uniform dark brown powder is obtained.

Methods. *X-Ray diffractometer (XRD).* XRD analysis was carried out using a D2 Phaser XRD diffractometer (Bruker, Germany) at room temperature. The samples were scanned over a Bragg angle (2θ) range of 10°–90°.

Fourier Transmission Infrared (FT-IR). Transmittance spectra were recorded in the wavenumber range of 400–4000 cm^{-1} using an IR Affinity-1 FT-IR spectrometer (Shimadzu, Japan).

Scanning Electron Microscopy (SEM). Morphology and elemental analysis were conducted using SEM Zeissevo(Zeiss, Germany) for analysis of the morphology of the synthesized NPs.

Transmission Electron Microscope (TEM). The morphology of the Al_2O_3 and CuO nanocomposite was observed with a high-resolution JEM-1400 (JEOL Ltd., Japan) equipped with a LaB6 electron gun and operating at an accelerating voltage of 80-120 kV.

The gamma radiation of nanostructured Al_2O_3 + CuO catalyst was carried out in a Co-60 (Cobalt-60) isotope device [24].

Characterization of Al_2O_3 and CuO nanoparticles. The results of XRD analysis of Al_2O_3, CuO, and Al_2O_3/12% CuO nanocomposite are shown in Fig. 1. The peaks observed at 31.7°, 37.8°,

45°, and 67° in the graph of pure Al_2O_3 are attributed to γ- phase of cubic spinel-structured Al_2O_3, and these phase crystallites correspond to the Müller indices of 220, 311, 400, and 440, respectively (JCPDS Card No. 29-0063). The relatively weaker peaks at 25.6°, 27.3°, 35.2°, 43.4°, 52.6°, 56.5°, 57.6°, and 75.5° indicate the appearance of α-Al_2O_3 NPs due to the temperature increase (Müller indices –012, 104, 113, 024, 116, and 1010, respectively). Crystallization of CuO NPs in a monoclinic structure was confirmed by XRD analysis. Intense peaks at angles of 35.5, 38.7, and 48.8 in the XRD spectrum indicate the presence of planes with Müller indices (111), (202), and (020), respectively. The XRD spectrum of the nanocomposite obtained by the addition of 12 wt% CuO to the γ -Al_2O_3 matrix shows that the intensity of the peaks belonging to γ -Al_2O_3 (at 31.7° and 45°) decreased several times, while the intensity of the peak at 37.8° of the matrix increased, on the contrary. The peak, which is seen as broad and very weak at 61.3° in the spectrum of γ -Al_2O_3 and relatively intense at 61.4° in the spectrum of CuO, appears at 60° in the spectrum of the Al_2O_3/12% CuO nanocomposite. Thus, we can assume that the addition of 12% CuO affected the arrangement of atoms in the crystal lattice of Al_2O_3, deforming the crystal lattice of the matrix to some extent.

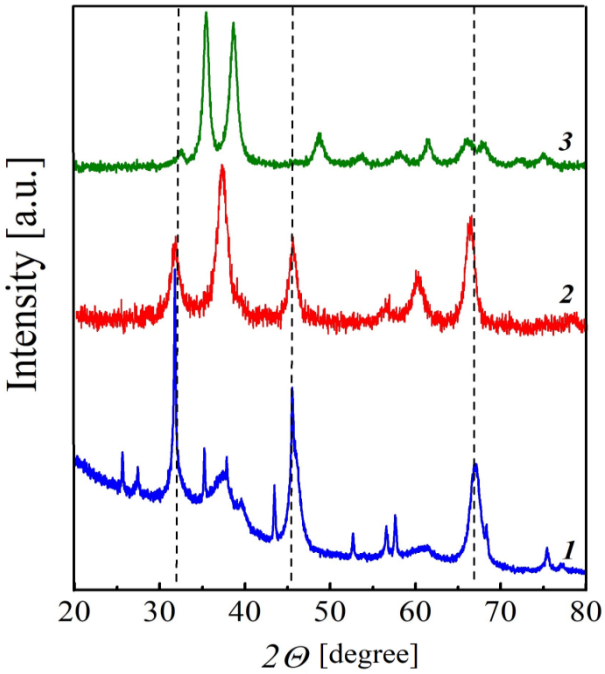

Fig. 1. XRD spectra of 1– Al_2O_3 , 2– CuO (2) NPs and 3–Al_2O_3/12%CuO nanocomposite

The results of XRD analysis were used to calculate the crystallite size of Al_2O_3 and CuO NPs according to the full width at half maximum of the peaks using the Scherer formula:

$$t = \frac{0.9\lambda}{B cos\theta} \qquad (1)$$

Where t is the crystal size, λ is the X-ray wavelength, B is the half-maximum of the peaks in spectrum, and θ is the Bragg angle. The calculated crystallite sizes of the CuO, γ-Al_2O_3 and α-Al_2O_3 nanoparticles synthesized by the sol-gel method were found within 8-10 nm, 5-8 nm and 37 nm, respectively.

Fig. 2 indicates the result of SEM analysis. As it can be seen from the figure, small nanoparticles of γ-Al_2O_3 can be clearly seen on large agglomerates (mesoporous structure of α-Al_2O_3).

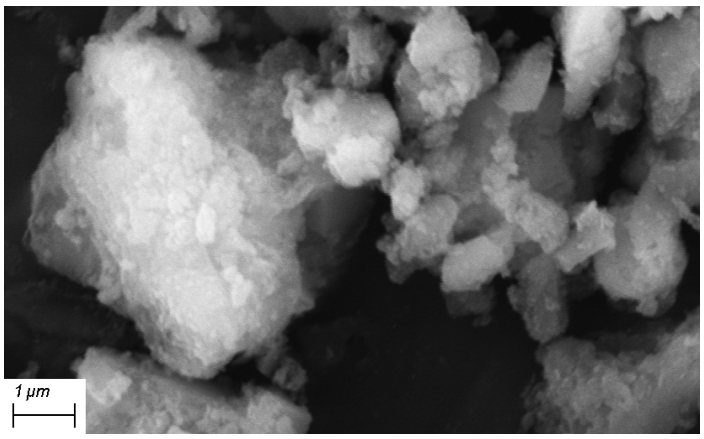

Fig. 2. SEM image of nanostructured Al_2O_3

A TEM micrograph of the Al_2O_3/12%CuO nanocomposite is shown in Figure 3, which illustrate a detailed view of its morphological structure. Both Al_2O_3 and CuO oxides in the composite exhibit a spherical shape, with particles showing a remarkable uniformity in size, which demonstrates a well-controlled synthesis process. The nanoparticle size observed in the TEM image aligns closely with the measurements obtained from XRD analysis, further confirming the consistency of the results across different characterization techniques. It is evident from the image, that the nanoparticles are arranged in close proximity to each other, forming a compact structure. Such a structure suggests that the particles tend to aggregate due to van der Waals interactions [23].

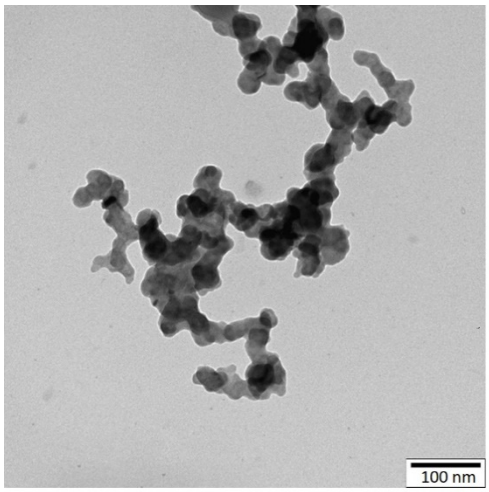

Fig. 3. TEM micrograph of the γ-Al_2O_3/CuO nanocomposite

The IR spectra of samples (Fig. 4) were investigated by FT-IR spectroscopy using an IR Affinity- 1 FT-IR device (Shimadzu, Japan). Samples for FT-IR analysis were prepared with high purity KBr powder. The FT-IR spectra of the synthesized nanoparticles and their composites are shown in Fig. 4. The peaks observed within 400-1000 cm^{-1} (489, 591, 780 cm^{-1}) show the Al-O vibration, confirmig the formation of the γ- Al_2O_3 phase and the peaks observed at 3200-3600 cm^{-1} interval show the vibration of the O-H stretching. More intense peaks at 1407 and 1627 cm^{-1} confirmed the existance of symmetrical stretching and bending vibrations of Al-O, respectively [25].

The peaks at 518 and 601 cm^{-1} in CuO IR spectrum are assigned to the Cu-O stretching vibration and confirms monoclinic structure of nanocrystals. The peak which corresponds to 1401 cm^{-1} in CuO nanoparticle spectrum with 12 % percentage of composites is shifted to 1405 cm^{-1}. It can be explained by stronger (intensive) vibration of Al-O compared to Cu-O. This also can be explained by the fact that compared to Al_2O_3 nanocrystals, the nanocrystals of CuO are more sensitive to air humidity [26].

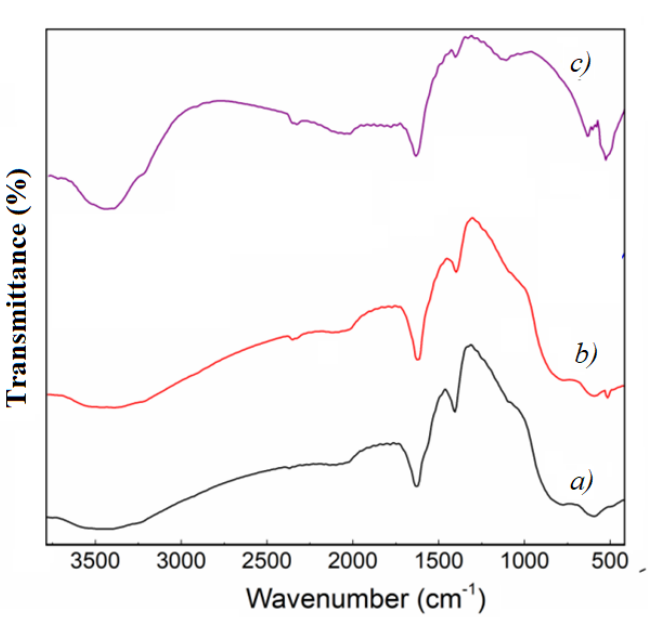

Fig. 4. FT-IR spectra of a) γ -Al_2O_3; b) γ -Al_2O_3-(12wt%CuO); c) CuO nanoparticles

The conversion of carbon monoxide (CO) to carbon dioxide (CO_2) was studied in three catalytic systems using Al_2O_3, mixed Al_2O_3/12%CuO and radiation-modified Al_2O_3/12%CuO nanocatalysts. For the experiment, nanocatalyst was taken with a catalyst total weight of m=7.32 grams (5.68+1.64 g). The experiments were carried out in the presence of oxygen at a dose rate of P=0.158 Gy/sec and different irradiation times. The main goal of the initial modification of the catalyst was to reach its highest activity rate in the conversion process and increase the radiation endurance of emerged centers to extend the lifetime of catalysts [20].

The catalytic oxidation of CO was carried out in a closed-loop flow reactor shown in Fig. 5.

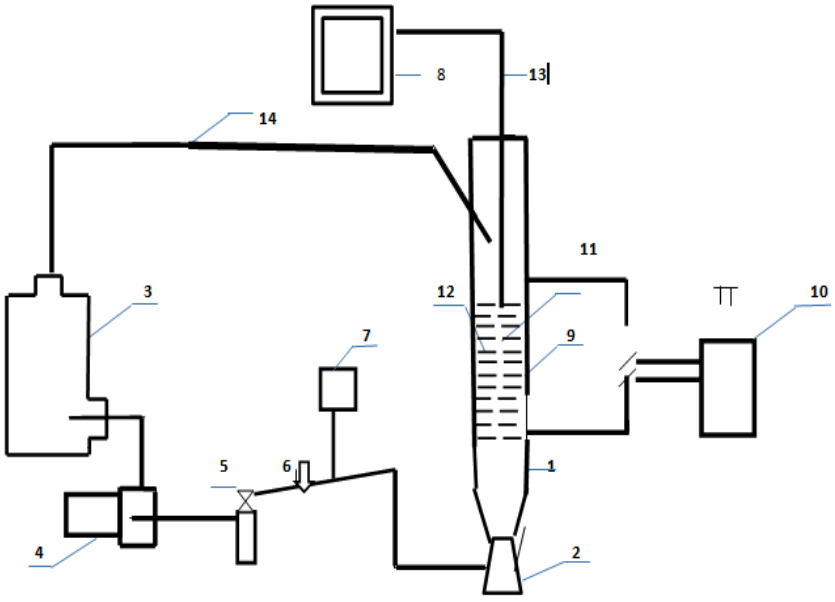

Fig. 5. Schematic diagram of closed-loop system for the catlytic conversion of CO to CO_2

1. Quartz reactor; 2. drop catcher; 3. an air-gas mixture cylinder with 5 liter volume; 4. compressor; 5. speed controller; 6. gas sampling point; 7. testo-301 gas analyzer; 8. thermocouple-M2020; 9. heating furnace of reactor; 10. tension regulator; 11. filter mesh; 12. nanocatalyst; 13. thermocouple; 14. connecting pipes.

The closed-loop system with a volume of 100 cm^3 quartz reactor is filled with the required amount of nano-catalyst (12). A filter mesh (11) was used to prevent the catalyst loss. The

temperature of the catalyst surface was controlled with a thermocouple millimeter –M2020 (13). The quartz reactor (1) is placed inside the heating furnace (9) so that the desired temperature can be obtained on the catalyst surface by changing the voltage supplied to the furnace with the tension regulator (10) connected to the circuit. The air-gas mixture (3) ($CO:O_2$)was injected onto the catalyst surface by compressor (4). The compressor simultaneously circulates the gas mixture in a closed system. Gas products and gas mixture converted on the catalyst surface at a given temperature are transferred to the drop catcher (2). Drop catcher also traps additional contamination in the system. $CO:CO_2$:NOx gases are monitored by Testo-301(7) installed on the gas mixture line leaving the system. At the same time, gas samples taken from the gas flow by sampler (6) are analyzed by Gaschrom chromatograph-3101 and the "Agilent Technologies 7890A GC" device J&W 113-4332,260 C, 30 m x 320 µm x 0 µm column. In the closed circuit scheme, the gas velocity is controlled by a 5-speed meter, and the given gas velocity is regulated from here. All these systems are interconnected by 10 mm plastic heat-resistant pipes (14). The experiments were carried out at temperatures within 70-350°C.

Results and Discussion

The values of experimental dependencies derived from the research have shown that the degree of oxidation/conversion of CO on the surface of nanocatalysts increases with the temperature increase in all three cases. A comparison of the dependences obtained for each experiment is shown in Fig. 6, where N/N_0 is the ratio of the initial (N_0) and outlet (N) amounts of CO and $1 - (N/N_0) \times 100$ is its conversion rate. R denotes the radiation-modified Al_2O_3/CuO nanocomposite.

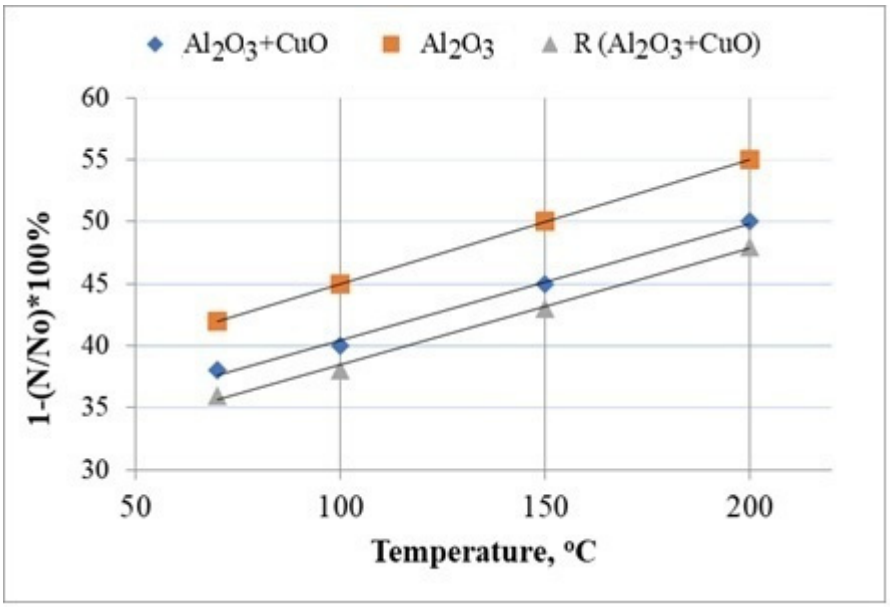

Fig. 6. Comparison of the temperature dependence of CO conversion to CO_2 on the surface of nanocatalysts.

Fig. 6 indicates that the degree of CO conversion increases approximately linearly with increasing temperature for all three catalyst systems. However, the slopes of the conversion curves (tan α) differ for each sample, indicating variations in catalytic activity. The slope values were found to be tan α = 0.10 for pure Al_2O_3, 0.092 for Al_2O_3/12%CuO, and 0.085 for radiation-modified Al_2O_3/12%CuO. The decrease in slope is associated with the reduction in the activation energy and a corresponding increase in the reaction rate for the mixed and radiation-modified catalysts.

Al_2O_3+CuO nanoparticles were irradiated with gamma rays in air at room temperature and a radiation dose of P = 15.82 rad/sec for τ = 17 hours. As a result of irradiation, additional active anionic centers were formed on the surface of the catalyst. These active anionic centers increased the reaction rate, and the activation energy became negative. The activation energy was calculated using the

Arrhenius equation ($k = A \exp(-E_a / RT)$, where E_a represents the activation energy). Thus, E_{Al2O3} = -6.68 kC/mol, $K_0 = 5.23 * 10^7$ sec^{-1}. The oxidation of CO on the catalyst surface has a lower activity in mixed copper oxide: $E_{Al2O3 + CuO}$ = -6.89 kC/mol, $K_0 = 5.23 * 10^7$ sec^{-1}, and with the initial modification of the surface under the influence of radiation, the activity is even lower, amounting to negative $E_{R\text{-}Al2O3 + CuO}$ = -7.23 kC/mol, $K_0 = 5.23 * 10^7$ sec^{-1}. In the high-temperature range, the radiation-catalytic homomolecular process leads to a negative activation energy for all the oxides studied. It should be noted that in figure 6, the activity of the radiation-modified catalyst appears to be low, which corresponds to a negative value of the activation energy.

At a reaction time of $\tau = 15$ min. and a temperature of 70 °C, the CO conversion rate – $1- (N/N_0) \times 100$ was 35% for pure Al_2O_3, 37% for Al_2O_3 + CuO, and 42% for radiation-modified Al_2O_3 + CuO. These results indicate that catalyst modification through CuO incorporation and surface radiation treatment enhances catalytic activity, leading to an increase in CO conversion rate by approximately 7–8% compared with the unmodified catalysts.

At higher temperatures, the effects of thermal activation and radiation-induced enhancement become comparable. As a result, the additional contribution of radiation modification diminishes, and the differences in CO conversion among the catalysts become insignificant.

The experimental results have shown that during the research the oxidation curves of CO are linear or arc-shaped.

The Langmuir-Hinshelwood equations are used to calculate the reaction rate by processing the experimental curves. Such dependencies are usually calculated in the stoichiometric ratio between CO and oxygen adsorbed on the active centers of the catalyst surface [27]. Depending on the concentration ratio of the components used, higher concentrations of particles are usually adsorbed to the catalyst surface, which plays a leading role in the activation of these molecules in the active centers and the subsequent oxidation processes. If CO is initially adsorbed on the surface, active oxygen atoms combine with it to form CO_2, and the rate of such reactions is expressed in the following formula:

$$W = \frac{kC_{co}\ C_{O_2}}{(1+KC_{co})2}$$

where: C_{co} and C_{O_2} are the concentrations of carbon monoxide and oxygen in the gas mixture measured in mole ratios, mol/mol;
k is the rate constant that depends on the temperature function, sec-1;
K is the equilibrium constant for the adsorption/desorption of CO on the active centers of the catalyst, depending on the temperature, (-).

The adsorption heat is sufficiently high ($Q_{ads.}$=140 kC/mol), and therefore, at high temperature, this value does not play a significant role in the course of the reaction. In the conditions of this investigation, since the concentration of the initial oxygen taken is many times greater than the concentration of carbon monoxide, the reaction rate depends only on the change of CO concentration, which makes this type of reaction a “pseudo” first-order reaction. The average activation energy of the processes calculated according to the Arrhenius equation is numerically small (ΔE =1.7 kcal/mol), confirming that the process occurs due to nanocatalytic action.

Fig. 7 shows that the decomposition curves are linear in all temperature ranges, corresponding to one-order reactions, with pseudo-rate constants k_1=(3.9÷9.3)10-3 varying in the range of 1/sec. For one-order reactions, along with rate constants, the half-conversion ($\tau_{1/2}$) quantity is also used, where $\tau_{1/2}$=(0.6936/ k_1) means the decomposition of half of the conventionally unit initial substance (t= $\tau_{1/2}$; C=C_0/2). This experiment shows that since the excess oxygen coefficient is equal to 1.2, the ratio of oxygen and carbon monoxide is determined to be close to stoichiometry.

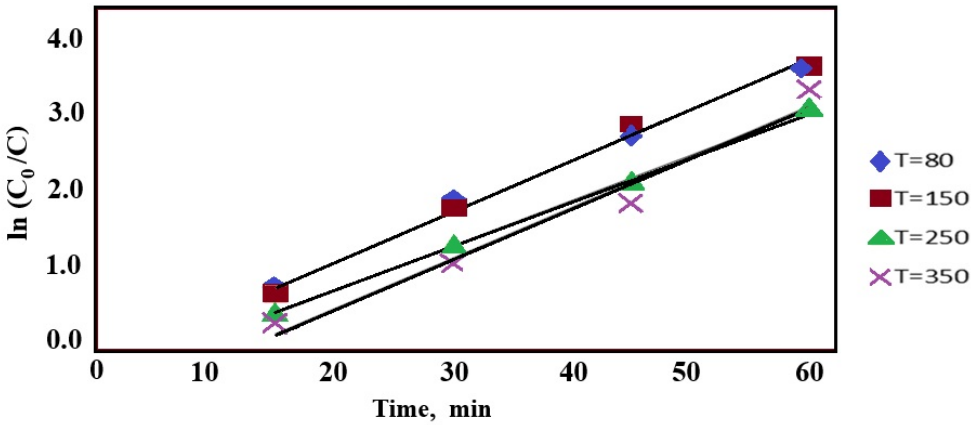

Fig. 7 Linear anamorphosis of carbon monoxide decomposition at different temperatures

Mechanism of processes on the catalyst surface. The Langmuir–Hinshelwood mechanism describes heterogeneous catalysis in which two or more reactants adsorb onto the catalyst surface, react with each other as adsorbed intermediates, and subsequently desorb as products. In this mechanism, the surface reaction is often the rate-determining step. It is a fundamental model in surface chemistry that explains how solid catalysts accelerate reactions by bringing reactants together on active sites, with reaction kinetics depending on surface coverage and adsorption behavior [28, 29].

Initially, the catalytic process proceeds through the adsorption of gaseous CO and O_2 on the catalyst surface and surface metal atoms. In a CO–O_2 mixture, carbon monoxide is the more active component. Therefore, it is preferentially adsorbed on coordinatively unsaturated metal atoms and, with the participation of surface vacancy defects, forms $CO\sigma–M\sigma^-$ complexes. Our earlier studies have shown that for CuO-containing catalysts in the CO neutralization reaction, the Cu^+–CO carbonyl complex acts as a key intermediate. Cu^{2+} cations interacting with CO molecules are readily reduced to Cu^+ cations, even at room temperature. These findings indicate that the Cu^+–CO complex is very stable and highly active in the catalytic conversion of CO to CO_2 [22].

During the initial irradiation of the system (gas mixture + catalyst), the energy absorbed by the catalyst creates electron-hole centers on the surface and in the volume, in other words, in the valence and conductivity bands. As a result, additional energy (in an amount equal to the energy of the valence band) is transferred to the surface, due to which oxygen molecules adsorbed on the surface are ionized, increasing the concentration of anionic centers (O^-) at the catalyst-gas mixture interface. Ultimately, the oxidation-reduction reactions that can occur on the catalyst surface are accelerated by the additional anionic sites formed at the interface.

The formation of these additional anionic centers accelerates oxidation–reduction reactions on the catalyst surface. In the subsequent stage, surface CO_2^{2-} anions are released through recombination with electrons from the valence band and hole centers on the catalyst surface. Finally, CO_2 desorbs from the catalyst surface as an electrically neutral molecule, making the overall process of CO oxidation to CO_2 highly efficient.

Conclusion

A composite Al_2O_3/CuO nanocatalyst was successfully synthesized and applied for the neutralization of carbon monoxide gas. The oxide nanoparticles were prepared using the sol–gel method, enabling the formation of highly dispersed CuO species on the Al_2O_3 support. The structural, morphological, and compositional properties of the synthesized materials characterized by XRD, FT-IR, SEM, and TEM techniques confirm the successful formation of both the composite nanocatalyst and the nanoscale distribution of the active components.

Catalytic activity studies demonstrated that the use of nanosized materials significantly enhances CO oxidation efficiency due to the increased specific surface area and the availability of a

greater number of active sites. Experimental results revealed that CO oxidation to CO_2 on the radiation-treated Al_2O_3/CuO nanocatalyst proceeds approximately 6–8% faster compared to the thermally activated process under identical conditions.

The observed enhancement in reaction rate is attributed to the formation of additional anionic centers on the catalyst surface induced by radiation exposure. These centers originate from ionized oxygen species (O^-), which act as highly active oxidizing agents. The presence of such surface oxygen anions promotes the adsorption and activation of CO molecules, facilitating their rapid oxidation to CO_2.

During the catalytic process, the active O^- species react with adsorbed CO to form CO_2, which subsequently desorbs from the catalyst surface. The oxygen anions are then replenished through interaction with gaseous oxygen, allowing them to participate repeatedly in successive catalytic cycles. This regenerative behavior of surface oxygen species ensures sustained catalytic activity and highlights the important role of radiation-induced surface modifications in enhancing the performance of Al_2O_3/CuO nanocatalysts for CO oxidation.

References

1. Parsazadeh B., Mahabadi H.A., Damyar N. Removal and determination of carbon monoxide based on copper oxide immobilized on Zeolite 13X Nanocatalyst by catalytic oxidation process and gas flow analyzer. *Anal. Methods Environ. Chem. J.*, 2023, **Vol. 6(4)**, p. 37-51. DOI: 24200/amecj.v6.i04.259
2. Khalilova H.Kh. The problems of the negative environmental impact of chemical pollutants and possible ways of their prevention. *Chemical Problems*, 2019, **Vol. 4(17)**, p. 500-517. DOI:10.32737/2221-8688-2019-4-500-517
3. Sassykova L.R., Aubakirov Y.A., Sendilvelan S., Tashmukhambetova Zh.Kh., Faizullaeva M.F., Bhaskar K., Batyrbayeva A.A., Ryskaliyeva R.G., Tyussyupova B.B., Zhakupova A.A., Sarybayev M.A. The Main Components of Vehicle Exhaust Gases and Their Effective Catalytic Neutralization. *Oriental Journal of Chemistry*, 2019, **Vol. 35(1)**, p. 110-127. http://dx.doi.org/10.13005/ojc/350112
4. Soliman N.K. Factors affecting CO oxidation reaction over nanosized materials: A review. *J. materrestechnol (jmr&t)*, 2019, **Vol. 8(2)**, p. 2395–2407. DOI: 10.1016/j.jmrt.2018.12.012
5. Moreno-Martell A., Pawelec B., Nava R., Mota N., Escamilla-Perea L., Navarro R.M., Fierro J.L.G. CO Oxidation at 20ºC on Au Catalysts Supported on Mesoporous Silica: Effects of Support Structural Properties and Modifiers. *Materials*, 2018, **no. 11**, 948. DOI:10.3390/ma11060948
6. Vershinin N.N., Balikhin I.L., Berestenko V.I., Efimov O.N., Kabachkov E.N., Kurkin E.N. Synthesis and Properties of a Carbon Monoxide Oxidation Catalyst Based on Plasma-Chemical Titanium Carbonitride, Titanium Dioxide, and Palladium. *High Energy Chemistry*, 2021, **Vol. 55(1)**, p. 75-79.
7. Aguila G., Gracia F., Araya P. CuO and CeO_2 catalysts supported on Al_2O_3, ZrO_2, SiO_2 in the oxidation of CO at low temperature. *Applied Catalysis*, 2008, **Vol. 343(1-2)**, p. 16-24. DOI: 10.1016/j.apcata.2008.03.015;
8. Sun S., Mao D., Yu J., Yang Zh., Lu G., Ma Zh. Low temperature CO oxidation on CuO/CeO_2 catalysts: the significant effect of CU precursor and calcination temperature. *Catal. Sci. Technol*., 2015, **no. 5**, 3166. DOI: 10.1039/c5cy00124b;
9. Zulfugarova S.M., Azimova G.R., Aleskerova Z.F., Tagiev D.B. Cobalt-containing oxide catalysts obtained by the sol-gel method with auto-combustion in the reaction of low-temperature oxidation of carbon monoxide. *Turkish Chemical Society (JOTCSA),* 2023, **no. 10**, p. 577-588. DOI: 10.18596/jotcsa.1261839
10. Li G., Feng W., Luo Y., Yan J., Cai Y., Wang Y., Zhang Sh., Liu W., Peng H. Unraveling FeOx Nanoparticles Confined on Fibrous Mesoporous Silica Catalyst Construction and CO Catalytic Oxidation Performance. *Catalysts*, 2024, **no. 14**, 63. DOI: 10.3390/catal14010063

11. Tan K., Zhang M., Shi J., Shan H., Liu H., He X., Cheng R., Zhao L., Zuo Sh., Yang P. Construction of CuO based composite oxide with high efficiency performance in catalytic degradation of toluene and chlorobenzene. *Ecotoxicology and environmental safety*, 2025, **Vol. 306**, 119336. DOI: 10.1016/j.ecoenv.2025.119336
12. Musayeva N., Khalilova H., Izzatov B., Trevisi G., Ahmadova Sh., Alizada M. Highly Selective Detection of Hydrogen Sulfide by Simple Cu-CNTs Nanocomposites. *Journal of Carbon research (C),* 2023, **no. 9**, 25. DOI:10.3390/c9010025
13. Zhang X., Zheksenbaeva Z.T., Sarsenovab R.O., Tungatarova S.A., Baizhumanova T.S., Zhevnitskiy S.I. Oxide Ni-Cu Catalysts for the Purification of Exhaust Gases. *Chemical engineering transactions*, 2020, **Vol. 81**, p. 925-930. DOI:10.3303/CET2081155
14. Dey S., Dhal G.Ch. Catalytic conversion of carbon monoxide into carbon dioxide over spinel catalysts: An overview. *Materials Science for Energy Technologies*, 2019, **no. 2**, p. 575-588. DOI: 10.1016/j.mset.2019.06.003
15. Di Benedetto A., Landi G., Lisi L. Improved CO-PROX Performance of CuO/CeO_2 Catalysts by Using Nanometric Ceria as Support. *Catalysts*, 2018, **no. 8**, 209. DOI:10.3390/catal8050209
16. Zhang Y., Zhao F., Yang H., Yin S., Wu C.-E, Zhou T., Xu J., Xu L., Chen M. Constructing Efficient CuO-Based CO Oxidation Catalysts with Large Specific Surface Area Mesoporous CeO_2 Nanosphere Support. *Nanomaterials*, 2024, **no. 14**, 485. DOI: 10.3390/ nano14060485
17. Hasanov S.H., Mahmudov H.M., Mustafayev I.I. The kinetics of convertation of carbon monoxide to carbon dioxide on the surface of mixed nano-catalyst in the closed system. *International Journal of Scientific & Engineering Research*, 2017, **Vol. 8(3)**, p. 1389-1393.
18. Li G., Feng W., Luo Y., Yan J., Cai Y., Wang Y., Zhang Sh., Liu W., Peng H. Unraveling FeOx Nanoparticles Confined on Fibrous Mesoporous Silica Cata Wang lyst Construction and CO Catalytic Oxidation Performance. *Catalysts*, 2024, **no. 14**, 63. DOI: 10.3390/catal14010063;
19. Dayan A., Alter J., Fleminger G. Catalytic Decontamination of Carbon Monoxide Using Strong Metal–Support Interactions on TiO_2 Microparticles. *Catalysts*, 2024, **no. 14**, 622. DOI: 10.3390/catal14090622
20. Hasanov S.H., Mustafayev I.I., Mahmudov H.M., Suleymanov T.Y., Huseyinova S.A. The influence of mixed nano-Al_2O_3+CuO catalysts that are initial radiation in air environment on the surface impact in the oxidation processes. *Radiation Effects and Defects in Solids*, 2019, DOI: 10.1080/10420150.2019.1665042
21. Vershinin N.N., Balikhin I.L., Kabachkov E.N., Kurkin E.N. Studying the Effect of Ultraviolet Irradiation on the Properties of a Carbon Monoxide Oxidation Catalyst Based on Titanium Dioxide, Plasma-Chemical Titanium Carbonitride, and Palladium. *High Energy Chemistry*, 2025, **Vol. 59(2)**, p. 167–172. DOI: 10.1134/S0018143924701789
22. Soltanov R.I., Khalilova H.Kh. Neutralization of NOx and CO gases using oxide and zeolite catalysts. Identification and characterization of Lewis acidic sites and carbonyl complexes. *J. Ecoenergetics*, 2025, **no. 1**, p. 12-14.
23. Khalilova H., Musayeva N., Nurubeyli T., Kashkay A., Rzayev F., Izzatov B., Aliyev M. Effectiveness of alumina/copper oxide nanocomposites in removing cadmium ions from aqueous solutions. *Composite Interfaces*, 2025, **Vol. 32(11)**, p. 1487-1491. DOI: 10.1080/09276440.2025.2493474
24. Cunningham J.R. *Encyclopedia of Medical Devices and Instrumentation Cobalt-60 Units for Radiotherapy.* First published. 2006. DOI: 10.1002/0471732877.emd063
25. Fernandes E.P., Silva T.S., Carvalho C.M., Selvasembian R., Chaukura N., Oliveira L. M.T.M, Meneghetti S.M.P., Meili L. Efficient adsorption of dyes by γ-alumina synthesized from aluminum wastes: Kinetics, isotherms, thermodynamics and toxicity assessment. *J Environ. Chem. Eng.* 2021, **no. 9,** 106198. DOI: 10.1016/j.jece.2021.106198.
26. Varughese A., Kaur R., Singh P. Green synthesis and characterization of copper oxide nanoparticles using psidium guajava leaf extract. *IOP Conf. Ser.: Mater. Sci. Eng.*, 2020, **Vol. 961,** 012011. DOI: 10.1088/1757-899X/961/1/012011.

27. Fedyaeva O.A., Onuchina V.O. Catalytic oxidation of carbon monoxide. *Nauka, Mysl, Electronic periodical journal*, 2017, **no. 2**, p. 164-167. (in Rus).
28. Sitja G., Tissot H., Henry C.R. Particle size effect on the Langmuir-Hinshelwood barrier for CO oxidation on regular arrays of Pd clusters supported on ultrathin alumina films. *The Journal of Chemical Physics*, 2019, **Vol. 151(17)**, 174703. DOI: ff10.1063/1.5125572ff.
29. Subhashish D., Dhal G.Ch., Mohan D., Prasad R. Advances in transition metal oxide catalysts for carbon monoxide oxidation: a review. *J. Advanced composites and hybrid metals*, 2019, **Vol. 2(3),** DOI: 10.1007/s42114-019-00126-3